IEEE Access
Multidisciplinary | Rapid Review | Open Access Journal

Received March 14, 2021, accepted March 27, 2021, date of publication March 30, 2021, date of current version April 8, 2021.

Digital Object Identifier 10.1109/ACCESS.2021.3069795

Optimized VAA Based Synthesis of Elliptical Cylindrical Antenna Array for SLL Reduction and Beam Thinning Using Minimum Number of Elements

HEBA SOLIMAN DAWOOD, HEBA ALI EL-KHOBBY, MUSTAFA MAHMOUD ABD ELNABY, AND AMR HUSSEIN HUSSEIN

Department of Electronics and Electrical Communications Engineering, Faculty of Engineering, Tanta University, Tanta 31527, Egypt

Corresponding author: Heba Soliman Dawood (hebadawood92@yahoo.com)

ABSTRACT In this paper, new virtual antenna array (VAA) based synthesis techniques are introduced for side lobe level (SLL) reduction, beam thinning, and number of elements minimization for elliptical cylindrical antenna arrays (ECAA) of radar systems. Thereby, significant improvements in the array gain and directivity are achieved, which enhance the detection range and angular resolution of the radar. Furthermore, the overall implementation cost of the system is highly reduced by saving the number of elements and the corresponding RF chains and simplifying the feeding network. Firstly, the proposed technique decomposes the single transmit/receive ECAA into a separate transmit linear antenna array (LAA) and receive elliptical antenna array (EAA). Secondly, the number of antenna elements, element spacing, and excitations of the created LAA and EAA are optimized using particle swarm optimization (PSO) to produce efficient beamformed patterns. Finally, the Kronker product of the optimized LAA and EAA patterns is performed to form the optimized virtual ECAA (V-ECAA) pattern. We also introduced both the uniform feeding based V-ECAA technique and the non-uniform feeding based V-ECAA synthesis technique for more flexibility and better productivity in antenna arrays design. The simulation results revealed that the uniform feeding based V-ECAA provides an identical pattern to that of the traditional uniform feeding ECAA while saves the number of elements by 66.6%. While in the case of non-uniform feeding based V-ECAA, it provides much lower SLL and narrower HPBW than those of the ECAA while saving the number of elements by 63.8%. Furthermore, the HB is applied to provide additional beam thinning and SLL reduction of the proposed non-uniform V-ECAA that is denoted as (HBV-ECAA). The possibility of practical validations of the synthesized V-ECAAs is verified using the computer simulation technology (CST) microwave studio package, which gives users an integrated design environment and achieves realizable and robust designs.

INDEX TERMS Elliptical cylindrical antenna array (ECAA), hyper beamforming (HB), virtual antenna array (VAA), particle swarm optimization (PSO), radar, side lobe level (SLL).

I. INTRODUCTION

Radar systems play an important role in every modern system. The main role of radar is to detect, measure the range, speed, and the direction of the surrounding objects. The radar requires a high directivity and high gain of antenna array system to be able to distinguish between nearby objects. This can be achieved by reducing the half power beamwidth (HPBW) and side lobe level (SLL) of its array radiation pattern. Many algorithms were introduced for linear antenna arrays (LAAs) synthesis such as are particle swarm optimization (PSO), BAT, real-value Genetic Algorithm (RGA), and method of moments/ genetic algorithm (MoM/GA) introduced in [1]–[4].

In [1]–[3], PSO and BAT optimization algorithms are used to improve the performance of LAAs in terms of reducing SLL, reducing HPBW, and directing nulls into particular directions by estimating the optimum values of the LAA excitation coefficients and element spacing. In [4], the hybrid MoM/GA array synthesis technique has been

The associate editor coordinating the review of this manuscript and approving it for publication was Chengpeng Hao.

used to synthesize the arbitrary shaped pattern LAAs with a minimum number of antenna elements. The analytical MoM technique is used to calculate the array excitation coefficients while the GA optimization technique is used to optimize the inter-element spacing of the array. This hybrid technique has proved superior performance compared to only optimization-based synthesis techniques.

For additional performance enhancement in terms of SLL and HPBW, the hyper beamforming (HB) is introduced in [5]–[7]. The HB mainly depends on the sum and difference beam patterns of the array that are raised to the hyper beam exponent to control the SLL and the HPBW. The HB has been applied on the uniform feeding LAA for SLL minimization where the excitation coefficients and the interelement spacing are optimized using the Firefly algorithm (FFA) [5], Seeker Optimization Algorithm (SOA) [6], and collective animal behavior (CAB) algorithm [7]. The simulation results revealed that the SOA provided the lowest SLL compared to that of FFA, RGA, and PSO. While the CAB provided better results in terms of SLL compared to that of RGA and PSO.

There is another trend for synthesizing antenna arrays using a fewer number of elements by using virtual antenna array (VAA) beamforming. The VAA concept is widely used in antenna array-based applications such as radar systems, multiple-input multiple-output (MIMO) systems, direction of arrival (DoA) estimation, and null broadening as introduced in [8]–[14]. In [8], the VAA has been used for MIMO synthetic aperture radar (SAR). Where, the VAA concept is applied on one-dimensional LAA for providing satisfied performance for remote sensing. While in [9], the combination of VAA and MoM/GA beamforming techniques has been introduced for the synthesis of medium-range radar (MRR) and long-range radar (LRR) PAA systems. The VAA is applied on a two-dimensional planar antenna array (PAA) by constructing two orthogonal LAAs. Where, the MoM/GA is used to estimate the excitation coefficients and the interelement spacing of the two orthogonal LAAs to provide the same radiation pattern as the original PAA.

In [10], [11], the modified virtual singular value decomposition (MV-SVD) algorithm and virtual array extension/matrix pencil method/genetic algorithm (VAE/MPM/GA) have been introduced, respectively. They are based on the VAA extension of small size antenna arrays to provide high DoA estimation accuracy. They extend the original antenna array size from M elements to virtual $(2M - 1)$ elements, which allows the system to identify more sources and provide higher resolution. In [12], a VAA-based DoA estimation technique has been introduced where the non-uniform feeding PAA is transformed into a uniform feeding virtual PAA consisting of a fewer number of elements. In addition, the VAA concept has been used for null broadening of antenna arrays as introduced in [13]. In [14], the VAA has been used to implement a hexagonal array configuration for MIMO radar. The hexagonal VAA based MIMO provided better results compared to perpendicular MIMO in terms of SLL, as it reduced the SLL by 3 dB.

It is worth mentioning that the elliptical cylindrical antenna array (ECAA) is one of the most commonly used antenna arrays in radar applications as introduced in [15]. The ECAA is a combination of a set of elliptical antenna arrays (EAAs) and LAAs. In [15], three ECAAs have been introduced including the uniform feeding ECAA, the non-uniform feeding ECAA, and the hyper beamforming (HB) based uniform and non-uniform feeding ECAAs. However, these array configurations have many drawbacks such as the utilization of a large number of antenna elements and RF front end chains, increased complexity of the feeding networks, increased overall system cost, and moderate SLL and HPBW which limit the detection range and resolution of the radar system.

In this paper, the performances of the three aforementioned ECAAs introduced in [15] are enhanced by using a hybrid combination between the VAA, PSO, and HB techniques. The VAA is used to decompose the single transmit/receive ECAA into a separate transmit LAA and a separate receive EAA for initial minimization of the number of antenna elements of the synthesized virtual ECAA (V-ECAA). In the case of uniform feeding V-ECAA, we perfectly implemented the desired uniform feeding ECAA pattern using a much fewer number of antenna elements. While in the case of non-uniform feeding V-ECAA, the PSO is used to optimize the excitation coefficients and element spacing of the constructed transmit LAA and receive EAA to synthesize high-performance V-ECAAs in terms of SLL and HPBW compared to the non-uniform feeding ECAA using minimum number of antenna elements. Furthermore, for more SLL reduction and beam thinning, the HB is applied to the proposed V-ECAA to introduce the HBV-ECAA synthesis technique, which achieved superior performance compared to hyper beamformed ECAA.

The key contributions of this paper are summarized as follows:

I Although the VAA principle is outdated for use in radar systems, the application of the PSO to the separate transmitter and receiver arrays which are the key components of the VAA prior to the Kronker product of their patterns is considered innovative. This is because the use of PSO guarantees optimal allocation and alignment of transmitter and receiver arrays, minimizes the required number of antenna elements, and optimizes both element spacing and excitation prior to the implementation of the VAA principle, which significantly enhances overall array system performance.

II This combination VAA/PSO allows the synthesis of the desired ECAA pattern with minimized number of antenna elements, which reduces the required number of RF front-end chains, simplifies the design of the feeding network, and reduces the overall system cost.

III In case of uniform feeding V-ECAA, the desired ECAA pattern is perfectly implemented while saving the number of elements by a ratio of 66.66%.

IV In case of non-uniform feeding V-ECAA, significant SLL reduction and beam thinning are achieved

compared to the non-uniform feeding ECAA while saving the number of elements by 63.8%.

V The proposed HBV-ECAA is able to reduce the SLL and narrow the HPBW compared to the hyper beamformed ECAA at different hyper beam exponent values.

VI In case of uniform feeding, the HBV-ECAA reduces the SLL by 345.32% and 140.99% compared to that of the hyper beamformed uniform ECAA at k= 0.1 and0.3, respectively.

VII In case of non-uniform feeding, the HBV-ECAA reduces the SLL by 18 dB, 29 dB, and 131 dB compared to that of the hyper beamformed non-uniform ECAA at $k = 0.5, 0.3$, and 0.1, respectively. Furthermore, it provides narrower HPBW by 4°, 0.9°, and 0.2° at $k = 0.5, 0.3$, and 0.1, respectively.

VIII The possibility of practical validations of designed V-ECAAs is verified using the well-known computer simulation technology (CST) microwave studio software package. The CST technology offers a more efficient approach to simulating both individual components and full systems, which gives users an integrated design environment. The designers can identify and resolve potential issues such as detuning, signal integrity (SI) and power integrity (PI) problems, and electromagnetic interference (EMI) at an early stage and thus obtain more robust and realizable designs.

The rest of the paper is organized as follows; in Section II, the problem formulation is presented in details, the PSO is introduced in Section III, the proposed VAA/PSO based synthesis techniques are presented in section IV, the hyper beamforming of the proposed V-ECAA is introduced in Section V, the simulation results and discussions are introduced in Section VI, and the conclusion is given in Section VII.

II. PROBLEM FORMULATION: TRADITIONAL ECAA

The ECAA is widely used in full duplex single antenna array based radar system. As shown in Fig. 1, the ECAA consists of M ellipses located in the X-Y plan and encircled around the Z- axis with vertical spacing d. All ellipses have the same major axis a and the same minor axis b. The N elements placed in a transversal plane constitute an elliptical antenna array (EAA). While the M elements aligned along the vertical line on the cylinder surface form a linear antenna array (LAA).

Thereby, the ECAA is a combination of N number of LAAs and M number of EAAs. The EAA pattern is expressed as [15]:

$$AF_{EAA}(\theta,\varphi) = \sum_{n=1}^{N} u_n e^{j(\beta \sin\theta.(a.\cos(\varphi)\cos(\varphi_n)+b.sin(\varphi)\sin(\varphi_n))+\mathrm{P}_n)} \quad (1)$$

where a and b are the major and minor axes of the ellipse, respectively, N is the number of the EAA elements, u_n is the excitation coefficient of the n^{th} element, β is the wave number, $\beta = 2\pi/\lambda$, and λ is the wavelength. θ is the elevation angle, φ is the azimuth angle, and φ_n is the angular position of the n^{th} element that is defined as:

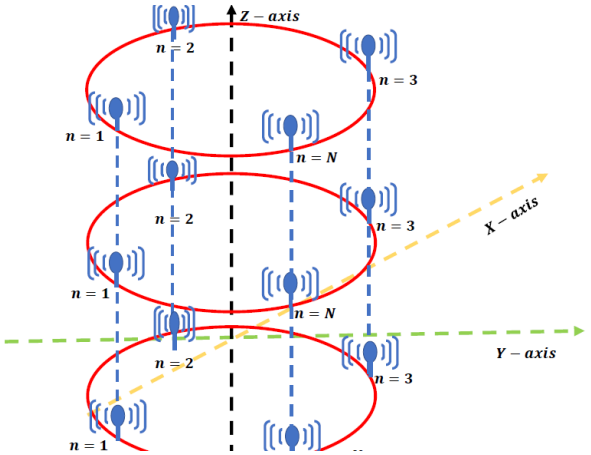

FIGURE 1. The ECAA geometry.

$$\varphi_n = 2\pi(n-1)/N \quad (2)$$

P_n is a parameter used to steer the main beam towards the desired direction as follows [15]:

$$\mathrm{P}_n = -\beta \sin\theta_0.(a.\cos(\varphi_0)\cos(\varphi_n) + b.sin(\varphi_0)\sin(\varphi_n)) \quad (3)$$

where θ_0 and φ_0 are the elevation angle and azimuth angle of the main beam, respectively.

On the other hand, the LAA pattern can be expressed as [15]:

$$AF_{LAA}(\theta) = \sum_{m=1}^{M} \upsilon_m e^{j\beta(m-1)d(cos\theta - cos\theta_0)} \quad (4)$$

where v_m is the excitation coefficient of the m^{th} antenna element.

The total ECAA pattern is obtained by combining the M number of EAA patterns as follows:

$$AF_{ECAA}(\theta,\varphi) = \sum_{m=1}^{M}\sum_{n=1}^{N} \times I_{mn} e^{j(\beta \sin\theta.(a.\cos(\varphi)\cos(\varphi_n)+b.sin(\varphi)\sin(\varphi_n))+\mathrm{P}_n)} \quad (5)$$

where I_{mn} is determined by:

$$I_{mn} = \upsilon_m e^{j\beta(m-1)d(cos\theta - cos\theta_0)}.u_n \quad (6)$$

For uniform feeding ECAA, u_n and υ_m are set to 1, where $n = 1, 2, \ldots, N$ and $m = 1, 2, \ldots, M$. However, the performance of the ECAA can be improved in terms of SLL and HPBW by using non-uniform feeding ECAA. In non-uniform feeding ECAA, υ_m of the elements of the LAAs are set to 1, while u_n of the EAAs elements are changed.

III. PARTICLE SWARM OPTIMIZATION (PSO)

Particle Swarm Optimization (PSO) is one of the metaheuristic optimization paradigms that is widely used in the last two decades. The PSO algorithm uses a swarm of particles, which traverse a multidimensional search space to reach to

the optima. It has the ability to solve the unsupervised applications and complex multidimensional problems. Also, it distinguishes by the low computational complexity, low required memory, and high accuracy features. In addition, PSO has many features over heuristic optimization algorithms such as GA: (i) PSO has two populations (best position and current position), thereby, it provides more diversity and exploration over a single population. (ii) It provides faster convergence and more variety in search trajectories. (iii) The efficiency of heuristic algorithms is highly dependent on the algorithm parameters and the number of variables [16].

In PSO, each state is considered as a unique particle with a position κ_i and velocity v_i at each iteration i. For each particle, the better position is realized by immediately updating its velocity and position considering its previous position and the previous best positions of the other particles. The velocity of the j^{th} particle at the i^{th} iteration is updated as follows [17]:

$$v_j^{i+1} = \left[\varpi \times v_j^i\right] + \left[u_1 \times rand\,(1,1) \times \left(\kappa_{gbest} - \kappa_j^i\right)\right] + \left[u_2 \times rand(1,1) \times \left(\kappa_{Pbest}^i - \kappa_j^i\right)\right] \quad (7)$$

while the position of the j^{th} particle at the i^{th} iteration is updated as follows:

$$\kappa_j^{i+1} = \kappa_j^i + v_j^{i+1} \quad (8)$$

where u_1 is the cognitive parameter, u_2 is the social parameter, ϖ is the inertia weight index, and *rand* (1, 1) is a MATLAB command that generates a random value within the range [0, 1]. ϖ organizes the influence of the previous velocity on the new velocity during the adjusting process. κ_{Pbest}^i is a best position of the particles in iteration i and κ_{gbest} is the global best position, which is considered as the best κ_{Pbest}^i through all iterations.

IV. PROPOSED VAA/PSO BASED SYNTHESIS TECHNIQUES OF ECAA

In this section, a VAA/PSO based synthesis technique denoted as V-ECAA is introduced for ECAAs synthesis using minimum number of antenna elements. The VAA concept is widely used in radar systems having separate transmit (TX) and receive (RX) antenna arrays. The resultant VAA pattern is the multiplication of the TX and RX arrays patterns [8], [9]. Thereby, the ECAA shown in Fig. 1 can be synthesized using the VAA concept as shown in Fig. 2 where the TX antenna array is formed as a LAA, while the RX antenna array is formed as a EAA. The transmit LAA has M_{Tx} elements which are placed on the Z-axis with uniform element spacing, d_s.

The transmit LAA pattern is given by:

$$AF_{TX}(\theta) = \sum_{m=1}^{M_{Tx}} q_m e^{j\beta(m-1)d_s(cos\theta - cos\theta_0)} \quad (9)$$

where q_m is the excitation coefficient of the m^{th} antenna element, $m = 1, 2, \ldots, M_{TX}$. While, the receive antenna array is designed as a single EAA consisting of N_{RX} elements and located in X-Y plan. The receive EAA pattern is given by:

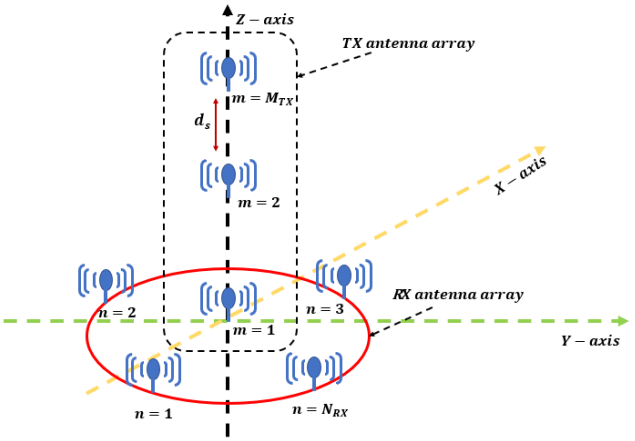

FIGURE 2. The geometry of the proposed V-ECAA.

$$AF_{RX}(\theta,\varphi) = \sum_{n=1}^{N_{RX}} \mathcal{P}_n e^{j(\beta \sin\theta.(a.\cos(\varphi)\cos(\varphi_n)+b.sin(\varphi)\sin(\varphi_n))+\mathrm{P}_n)} \quad (10)$$

where $\mathcal{P}_n$ is the excitation coefficient of the m^{th} antenna element, $n = 1, 2, \ldots, N_{RX}$. The V-ECAA pattern is obtained by the Kronker product of the transmit LAA pattern and the receive EAA pattern. The general expression of the V-ECAA pattern can be expressed as [8], [9]:

$$AF_{V-ECAA}(\theta,\varphi) = AF_{TX} \otimes AF_{RX} \quad (11)$$

where $\otimes$ is the Kronker product. In the following sections, both the uniform feeding V-ECAA (UV-ECAA) and the non-uniform feeding V-ECAA (NUV-ECAA) arrays are introduced.

A. ProposedUV-ECAA

In this section, the UV-ECAA is introduced to synthesize the same pattern as that of the uniform feeding ECAA. In this case, the excitation coefficients of transmit LAA and receive EAA (q_m and $\mathcal{P}_n$) are set to 1 in (9) and (10). While the number of elements N_{RX}, M_{TX} and the inter element spacing d_s are optimized using PSO to minimize the designed cost function $\mathcal{CF}_{UV}$ under the constraint that both the synthesized pattern $AF_{UV-ECAA}(\theta,\varphi)$ and the original pattern $AF_{ECAA}(\theta,\varphi)$ have the same HPBW as follows:

$$\mathcal{CF}_{UV} = \frac{1}{L}\sum_{l=1}^{L}[\|AF_{UV-ECAA}(l) - AF_{ECAA}(l)\|]^2|_{HPBW_{UV-ECAA}=HPBW_{ECAA}} \quad (12)$$

where L is the number of samples used to represent the array pattern, $HPBW_{UV-ECAA}$ and $HPBW_{ECAA}$ are the HPBWs of the synthesized UV-ECAA and the uniform feeding ECAA, respectively. It is worth mentioning that the minimization of the cost function corresponds to the minimization of the mean square error between $AF_{UV-ECAA}(\theta,\varphi)$ and $AF_{ECAA}(\theta,\varphi)$.

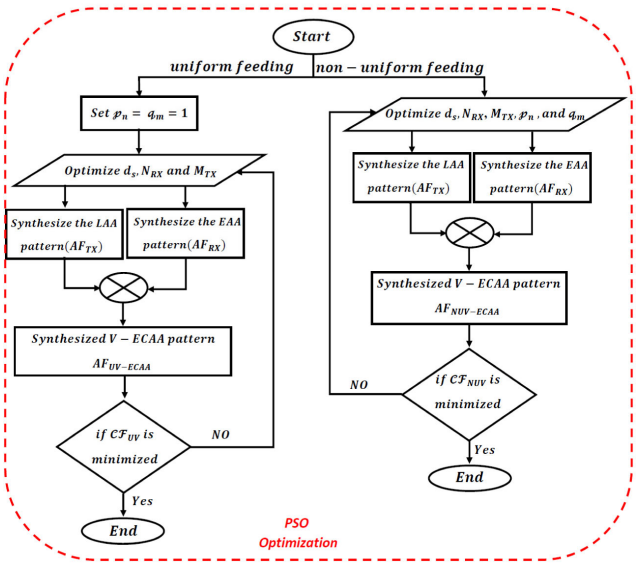

FIGURE 3. The flow chart of proposed UV-ECAA and NUV-ECAA synthesis techniques.

B. PROPOSED NUV-ECAA

In this section, the NUV-ECAA is introduced to improve the performance of the non-uniform feeding ECAA in terms of SLL and HPBW. In this case, both the excitation coefficients ($\mathcal{A}_m$ and $\mathcal{P}_n$), the number of elements (N_{RX} and M_{TX}), and the inter element spacing d_s are optimized using PSO to minimize the SLL of the $AF_{ECAA}(\theta, \varphi)$. The PSO determines the optimum values of $\mathcal{P}_n$, $\mathcal{A}_m$, N_{RX}, and M_{TX} to minimize the designed cost function, $\mathcal{CF}_{NUV}$.

$$\mathcal{CF}_{NUV} = 20log_{10} \left. \frac{\max(AF_{NUV-ECAA}(\theta_{SL}))}{AF_{NUV-ECAA}(\theta_0)} \right|_{HPBW_{NUV-ECAA} < HPBW_{ECAA}} \quad (13)$$

where θ_{SL} is the angle of the side lobe of the synthesized pattern $AF_{NUV-ECAA}(\theta, \varphi)$. The amplitude of the main beam at the main beam direction θ_0 is $AF_{NUV-ECAA}(\theta_0)$ and $HPBW_{NUV-ECAA}$ is the HPBW of the synthesized pattern $AF_{NUV-ECAA}(\theta, \varphi)$. Fig. 3 shows the flow chart, which describes the proposed UV-ECAA and NUV-ECAA synthesis techniques. To minimize the cost function CF_{NUV}, the amplitude of the main beam should be maximum and the amplitude of the maximum side lobe should be minimum under the constraint that the synthesized $HPBW_{NUV-ECAA}$ be less than that of the original non-uniform ECAA.

V. HYPER BEAMFORMING OF THE PROPOSED V-ECAA

In this section, the HB is applied to the proposed V-ECAA (HBV-ECAA) to provide additional SLL reduction and beam thinning. The HB concept is based on the generation of sum and difference patterns, which are raised to the power of a hyper beam exponent parameter. The sum pattern is obtained by taking the summation of the absolute values of left and right patterns. While, the difference is the absolute value of the difference between the left and right patterns. The right and left patterns are originated from dividing the antenna pattern crossing the x-axis. Starting from 0° going to the $-ve$ x-axis results in left pattern. While, the right pattern is obtained starting from 0° going to the $+ve$ x-axis [5]–[7]. The HB is applied only on the receive EAA, while the transmit LAA is kept unchanged.

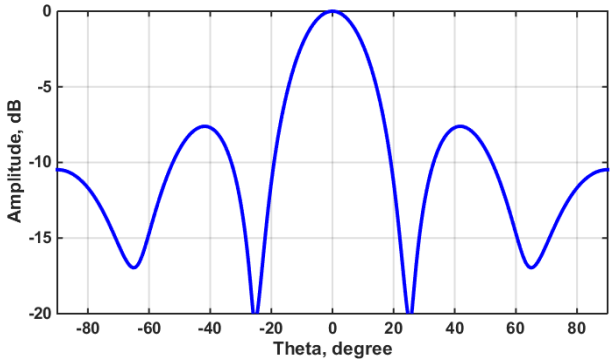

FIGURE 4. Sum pattern of 10 elements EAA.

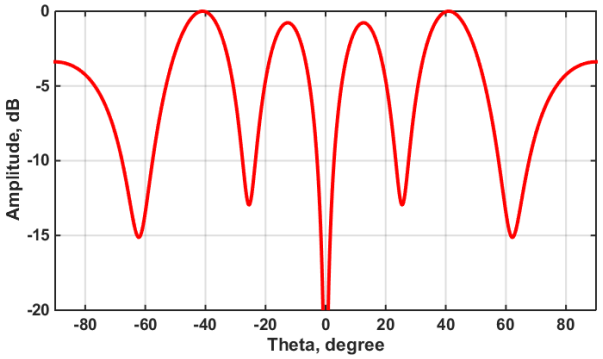

FIGURE 5. Difference pattern of 10 elements EAA.

The left pattern of the receive EAA is synthesized using the EAA elements from 1 to $\frac{N_{RX}}{2}$ as follows [5]–[7]:

$$AF_{RX-left} = \sum_{n=1}^{N_{RX}/2} \mathcal{P}_n e^{j(\beta \sin\theta.(a.\cos(\varphi)\cos(\varphi_n)+b.sin(\varphi)\sin(\varphi_n))+P_n)} \quad (14)$$

While, the right pattern of the RX antenna array is synthesized using the remaining elements from $\left(\frac{N_{RX}}{2}+1\right)$ to N_{RX} as follows [5]–[7]:

$$AF_{RX-right} = \sum_{n=\frac{N_{RX}}{2}+1}^{N_{RX}} \mathcal{P}_n e^{j(\beta \sin\theta.(a.\cos(\varphi)\cos(\varphi_n)+b.sin(\varphi)\sin(\varphi_n))+P_n)} \quad (15)$$

Then, the sum and difference patterns are generated as follows [5]–[7]:

$$AF_{RX-sum} = \left|AF_{RX-left}\right| + \left|AF_{RX-right}\right| \quad (16)$$

$$AF_{RX-diff} = \left|AF_{RX-left} - AF_{RX-right}\right| \quad (17)$$

Fig. 4 and Fig. 5 show examples for the sum and difference patterns generation from 10-elements EAA.

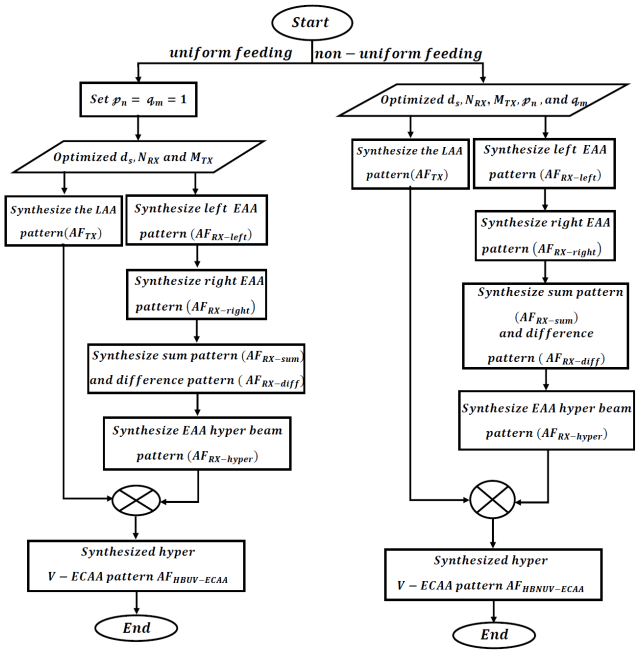

FIGURE 6. The flow chart of proposed HBUV-ECAA and HBNUV-ECAA synthesis techniques.

Consequently, the hyper beam pattern of the receive antenna array can be expressed as [5]–[7]:

$$AF_{RX-hyber} = \left((AF_{RX-sum})^k - \left(AF_{RX-diff}\right)^k \right)^{1/k} \quad (18)$$

where k is the hyperbeam exponent, which lies within the range $(0.1 : 1)$. If k equals 0.1, the $AF_{RX-hyber}$ pattern will have large spike depth towards the main beam direction. However, if k exceeds 1, the side lobes of the $AF_{RX-hyber}$ pattern will be higher than that of AF_{RX}. From (11), the synthesized pattern using the HBV-ECAA is written as follows:

$$AF_{HBV-ECAA} = AF_{TX} \otimes AF_{RX-hyber} \quad (19)$$

When HB applying is applied to the UV-ECAA, the synthesis technique is denoted as HBUV-ECAA. While in case of NUV-ECAA, it is denoted as HBNUV-ECAA. The flow chart of proposed HBUV-ECAA and HBNUV-ECAA techniques is shown in Fig. 6.

VI. SIMULATION RESULTS AND DISCUSSIONS

In this section, several simulations are carried out to verify the superiority of the proposed V-ECAA compared to the traditional uniform feeding ECAA (U-ECAA) and the non-uniform feeding ECAA (NU-ECAA). In addition, the superiority of the proposed HBV-ECAA compared to the hyper beamformed ECAA is verified. In the simulations, the proposed V-ECAA and HBV-ECAA are compared to the traditional U-ECAA and NU-ECAA introduced in [15], respectively at the same specifications listed in Table 1. The number of PSO iterations is denoted as N_{PSO}. The simulations results are divided into four sections as follows:

1) *UV-ECAA versus U-ECAA.*

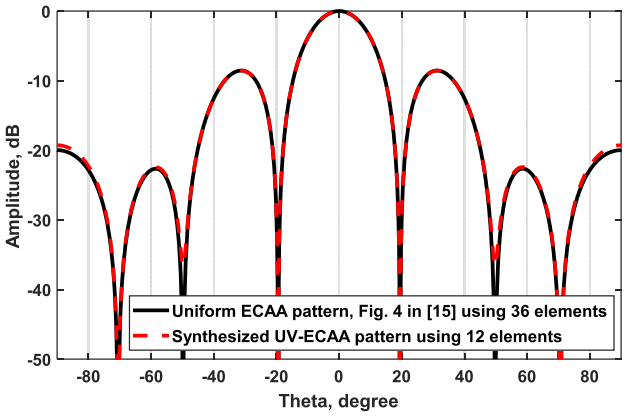

FIGURE 7. Rectangular plot of the U-ECAA pattern compared to the synthesized UV-ECAA pattern.

TABLE 1. Specifications of the traditional ECAA.

Parameter	*Value*
k	0.1 to 1
a	1.15
b	0.9959
f	305 MHz
θ_0	0°
φ_0	0°

2) *NUV-ECAA versus NU-ECAA*
3) *HBV-ECAA versus HB-ECAA.*
4) *Implementation of the Synthesized V-ECAAs Using CST Microwave Studio.*

A. UV-ECAA VERSUS U-ECAA

In this section, the proposed UV-ECAA is compared to the traditional U-ECAA that is generated using $M = 3$ and $N = 12$ elements as introduced in [15]. In this case, the U-ECAA is formed from 36 elements. Applying the proposed UV-ECAA technique, the rectangular plot of the U-ECAA and the UV-ECAA patterns are shown in Fig. 7. While, the PSO optimized values of N_{RX}, M_{TX}, d_s, N_{PSO}, and CF_{UV} are listed in Table 2. As shown in Fig. 7, it is clear that the proposed UV-ECAA provides an identical pattern to that of the U-ECAA. They have the same SLL and HPBW, which equal -8.5 dB and 17.82°, respectively. Furthermore, the UV-ECAA reduces the number of elements from 36 to only 12 elements such that; ($N_{RX} = 9$ elements are used to form the receive EAA and $M_{TX} = 3$ elements are used to form the transmit LAA). Accordingly, there is 66.6% saving in the overall number of antenna elements.

B. NUV-ECAA VERSUS NU-ECAA

In this section, the proposed NUV-ECAA is compared to the traditional NU-ECAA introduced in [15]. Performing the proposed NUV-ECAA, Fig. 8 shows the rectangular plot of the synthesized NUV-ECAA pattern compared to the NU-ECAA pattern. However, the PSO optimized values

TABLE 2. The optimized values of N_{RX}, M_{TX}, N_{PSO}, and $\mathcal{CF}_{UV}$.

Parameter	*Value*
N_{RX}	9
M_{TX}	3
d_s	$0.5\,\lambda$
N_{PSO}	60
$\mathcal{CF}_{UV}$	$9.8676 * 10^{-6}$

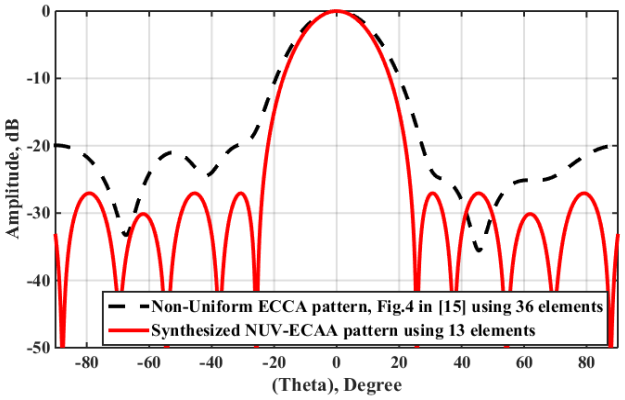

FIGURE 8. The rectangular plot of the NU-ECAA pattern compared to the synthesized NUV-ECAA pattern.

TABLE 3. The optimized values of N_{RX}, M_{TX}, N_{PSO}, and $\mathcal{CF}_{NUV}$.

Parameter	*Value*
N_{RX}	10
M_{TX}	3
d_s	$0.7\,\lambda$
N_{PSO}	284
$\mathcal{CF}_{NUV}$	-27 dB

TABLE 4. A comparison between the NUV-ECAA pattern and the NU-ECAA pattern in terms HPBW, SLL, and number of elements.

Parameter	NU-ECAA	NUV-ECAA
HPBW	22°	18.7°
SLL	-20 dB	-27 dB
Number of elements	36	13

of N_{RX}, M_{TX}, d_s, N_{PSO}, and $\mathcal{CF}_{NUV}$ are listed in Table 3. A comparison between the NUV-ECAA and the NU-ECAA patterns in terms HPBW, SLL, and number of elements is listed in Table 4. The optimum values of $\mathcal{q}_m$ and $\mathcal{p}_n$ are listed in Table 5. While, the excitation coefficients of the NU-ECAA are listed in Table 6. By analyzing the results, it is clear that the NUV-ECAA pattern provides better performance than the NU-ECAA pattern in terms of SLL and HPBW. It provides a 3.3° narrower HPBW than that of the NU-ECAA pattern. Also, it provides a 7 dB lower SLL than that of the ECAA pattern. Furthermore, it decreases the number of elements from 36 elements to 13 elements. Accordingly, the number of elements is reduced by 63.8%.

C. HBV-ECAA VERSUS HB-ECAA

In this section, the HB is applied on both the proposed UV-ECAA and NUV-ECAA for comparison with the hyper beamformed uniform ECAA (HBU-ECAA) and hyper beamformed non-uniform ECAA (HBNU-ECAA), respectively as follows:

TABLE 5. The optimum values of $\mathcal{q}_m$ and $\mathcal{p}_n$.

TX antenna array		RX antenna array			
M_{TX}	$\mathcal{q}_m$	N_{RX}	$\mathcal{p}_n$	N_{RX}	$\mathcal{p}_n$
1	0.7823	1	0.8413	6	0.8267
2	0.5	2	0.0158	7	0.0832
3	0.7478	3	0.9999	8	0.6188
		4	0.9638	9	0.6132
		5	0.0250	10	0.0508

TABLE 6. The excitation coefficients of the NU-ECAA (u_n).

N	u_n	N	u_n	N	u_n
1	0.0137	13	0.4542	25	0.3312
2	0.3474	14	0.0640	26	0.0379
3	0.5898	15	0.7398	27	0.6150
4	0.8857	16	0.6157	28	0.1633
5	0.6890	17	0.0129	29	0.2464
6	0.1843	18	0.0685	30	0.0686
7	0.5594	19	0.0130	31	0.1684
8	0.1517	20	0.0820	32	0.0332
9	0.0176	21	0.4318	33	0.1998
10	0.2440	22	0.7279	34	0.9919
11	0.0595	23	0.2761	35	0.3254
12	0.0088	24	0.0444	36	0.1496

TABLE 7. A comparison between the proposed HBUV-ECAA patterns and the traditional HBU-ECAA patterns.

k	Parameter	HBU-ECAA	HBUV-ECAA
0.1	HPBW	0.5°	0.5°
	SLL	-41.74 dB	-185.68 dB
0.3	HPBW	2°	2°
	SLL	-17.22 dB	-41.5 dB

1) HBUV-ECAA VERSUS HBU-ECAA

In this section, the HB is applied on the UV-ECAA introduced in section (VI. A) and on the U-ECAA introduced in [15] at $k = 0.1$ and 0.3. Fig. 9 and Fig. 10 show the rectangular plot of synthesized 12-elements HBUV-ECAAs and the HBU-ECAAs at $k = 0.1$ and 0.3, respectively. A comparison between the synthesized HBUV-ECAA patterns and the HBU-ECAA patterns is presented in Table 7. By analyzing the results, it is revealed that the HBUV-ECAA and the HBU-ECAA provides the same HPBW at $k = 0.1$ and 0.3. While, the HBUV-ECAA provides much lower SLL than that of the HBU-ECAA, as it reduces the SLL from -41.74 dB to -185.68 dB and from -17.22 dB to -41.5 dB at $k = 0.1$ and 0.3, respectively. Accordingly, the SLL is reduced by 345.32 % and 140.99%, at $k = 0.1$ and 0.3, respectively.

2) HBNUV-ECAA VERSUS HBNU-ECAA

In this section, the HB is applied on the NUV-ECAA introduced in section (VI. B) and on the NU-ECAA introduced

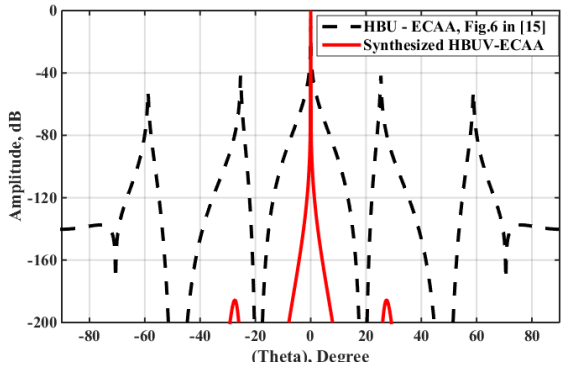

FIGURE 9. The rectangular plot of the HBU-ECAA pattern compared to the proposed HBUV-ECAA pattern at $k = 0.1$.

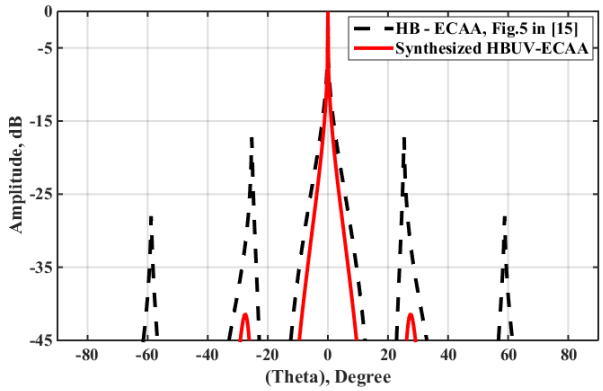

FIGURE 10. The rectangular plot of the HBU-ECAA pattern compared to the proposed HBUV-ECAA pattern at $k = 0.3$.

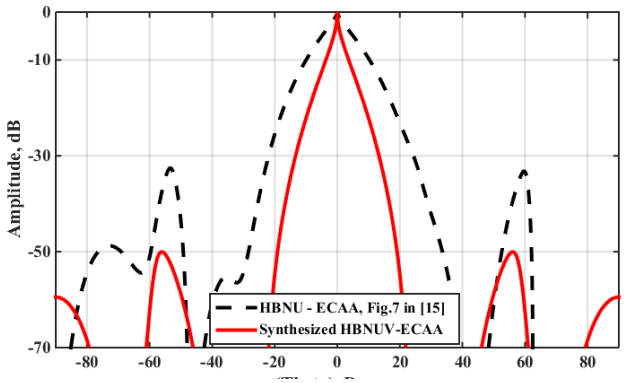

FIGURE 11. The rectangular plot of the HBNU-ECAA pattern compared to the proposed HBNUV-ECAA pattern at $k = 0.5$.

in [15] at different values of the hyper beam exponent k. The comparisons between the rectangular plots of the synthesized 13-elements HBNUV-ECAAs and the HBUN-ECAAs at $k = 0.1, 0.3$, and 0.5 are shown in Fig. 11, Fig. 12, and Fig. 13 respectively. While, a comparison between the proposed HBNUV-ECAA patterns and the HBUN-ECAA patterns is listed in in Table 8. The simulation results revealed that the proposed HBV-ECAAs provide better results in terms of SLL and HPBW than those of the HBUN-ECAAs at all values of k. They provide significant reductions in the SLL

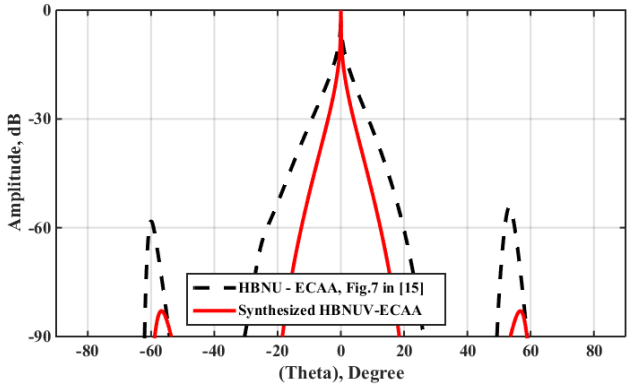

FIGURE 12. The rectangular plot of the HBNU-ECAA pattern compared to the proposed HBNUV-ECAA pattern at $k = 0.3$.

TABLE 8. A comparison between the proposed HBNUV-ECAA patterns and the traditional HBUN-ECAA patterns.

k	Parameter	HBNU-ECAA	HBNUV-ECAA
0.5	HPBW	6°	2°
	SLL	-32.5 dB	-50.5 dB
0.3	HPBW	1.8°	0.7°
	SLL	-54 dB	-83 dB
0.1	HPBW	0.3°	0.1°
	SLL	-139 dB	-270 dB

by 55.4%, 53.7%, and 94.2% at $k = 0.5, 0.3$, and 0.1, respectively. Also, they decrease the HPBW by 4°, 0.9°, and 0.2° at $k = 0.5$, 0.3, and 0.1, respectively. Furthermore, the number of elements, which is used to implement the HBV-ECAAs, is lower than that of the HBUN-ECAAs by 23 elements. Thereby reducing required RF front end channels, and hence reducing the overall system cost. By comparing the results in Table 4 to the hyper beamforming results in Table 8, it is clear that the HB plays an important role in SLL reduction and beam thinning. As, it decreases the SLL by 12.5 dB,34 dB, and 119 dB at $k = 0.5, 0.3$, and 0.1, respectively in case of HBNU-ECAAs. While in case of HBNUV-ECAAs, it decreases the SLL by 23.5 dB, 56 dB, and 243 dB at $k = 0.5, 0.3$, and 0.1, respectively. Also, it provides narrower HPBW by 16°, 20.2°, and 21.7° at $k = 0.5, 0.3$, and 0.1, respectively in case of HBNU-ECAAs. While in case of HBNUV-ECAAs, the HPBW is decreased by 16.7°, 18°, and 18.6° at $k = 0.5, 0.3$, and 0.1, respectively.

Finally, the simulation results of the V-ECAA compared to ECAA for uniform feeding, non-uniform feeding, and applying HB on them are summarized in brief in TABLE 9 which contains the computed SLL, HPBW, and number of elements.

D. IMPLEMENTATION OF THE SYNTHESIZED V-ECAAs USING CST MICROWAVE STUDIO

In this section, the synthesized V-ECAAs and the traditional ECAAs are implemented using CST Microwave Studio taking into account the effect of mutual coupling between the

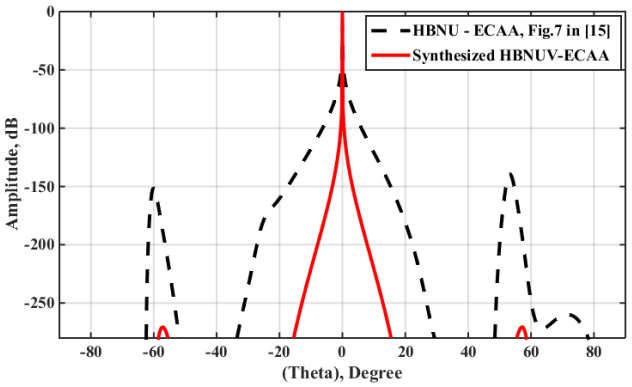

FIGURE 13. The rectangular plot of the HBNU-ECAA pattern compared to the proposed HBNUV-ECAA pattern at $k = 0.1$.

TABLE 9. A comparison between the proposed V-ECAA compared to ECAA at uniform feeding, non-uniform feeding, and after applying hyper beamforming.

Array	HPBW	SLL	Number of elements
U-ECAA	17.82°	−8.5 dB	36
UV-ECAA	17.82°	−8.5 dB	**12**
HBU-ECAAs at $k = 0.1$	0.5°	−41.74 dB	36
HBUV-ECAA at $k = 0.1$	0.5°	**−185.68 dB**	**12**
HBU-ECAA at $k = 0.3$	2°	−17.22 dB	36
HBUV-ECAA at $k = 0.3$	2°	**−41.5 dB**	**12**
NU-ECAA	22°	−20 dB	36
NUV-ECAA	**18.7°**	**−27 dB**	**13**
HBNU-ECAA at $k = 0.5$	6°	−32.5 dB	36
HBNUV-ECAA at $k = 0.5$	**2°**	**−50.5 dB**	**13**
HBNU-ECAA at $k = 0.3$	1.8°	−54 dB	36
HBNUV-ECAA at $k = 0.3$	**0.7°**	**− 83 dB**	**13**
HBNU-ECAA at $k = 0.1$	0.3°	− 139 dB	36
HBNUV-ECAA at $k = 0.1$	**0.1°**	**− 270 dB**	**13**

antenna elements. The mutual coupling affects the antenna characteristics drastically in terms of the SLL and main beam properties and therefore degrades the performance of the system [18], [19]. In this section, the V-ECAAs and ECAAs are implemented using a $\lambda/2$ dipole antenna radiating at resonance frequency $f_o = 0.305$ GHz. The dipole structure, H-plane, and E-plane patterns are shown in Fig. 14. While, the scattering parameter $|S_{11}|$ versus frequency of the dipole antenna is shown in Fig. 15. The patterns of the synthesized V-ECAAs are compared to those of the traditional ECAAs in terms of HPBW and SLL under practical conditions that have been adjusted in CST simulations. The CST simulations are divided into three sections as follows:

1) *CST Implementation of UV-ECAA versus U-ECAA.*
2) *CST Implementation of NUV-ECAA versus NU-ECAA.*
3) *CST Implementation of HBNUV-ECAA versus HBNU-ECAA.*

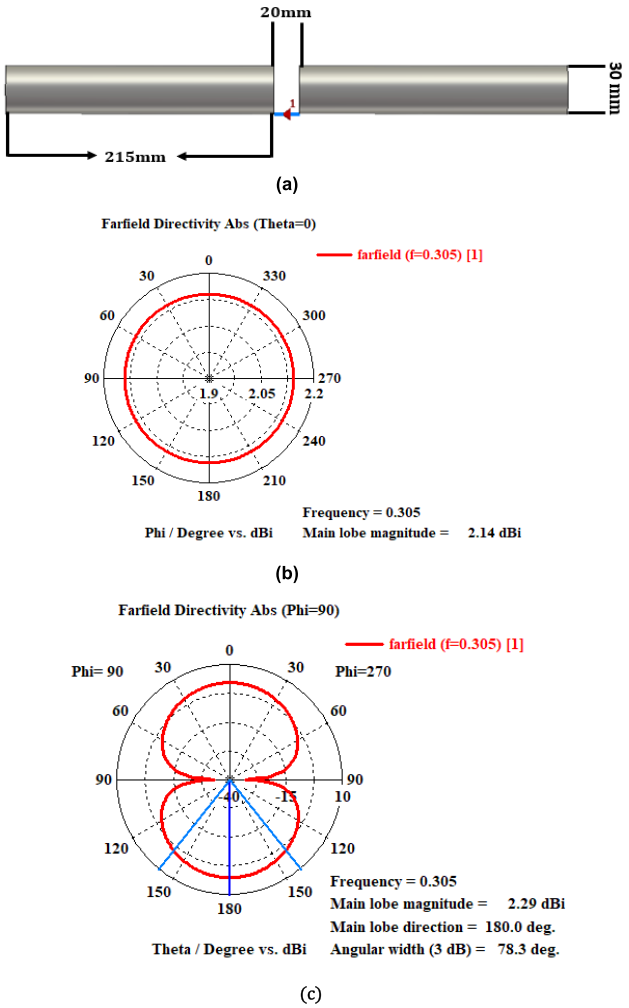

FIGURE 14. Dipole antenna: (a) dimensions, (b) H-plane pattern, and (c) E-plane pattern.

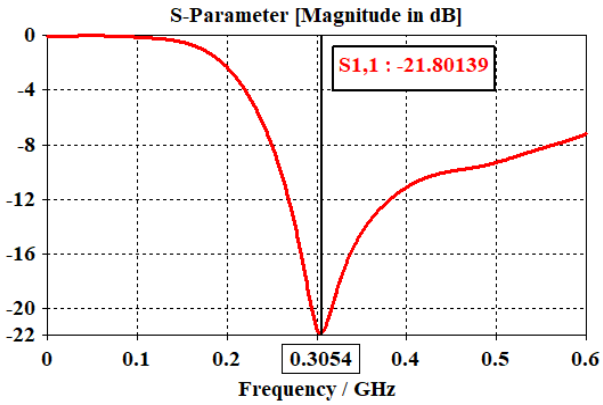

FIGURE 15. The scattering parameter $|S_{11}|$ versus frequency of the dipole antenna.

1) CST IMPLEMENTATION OF UV-ECAA VERSUS U-ECAA

In this section, the 12-elements UV-ECAA and 36-elements U-ECAA arrays presented in section (IV.A) are implemented using CST as shown in Fig. 16. The rectangular plots of their

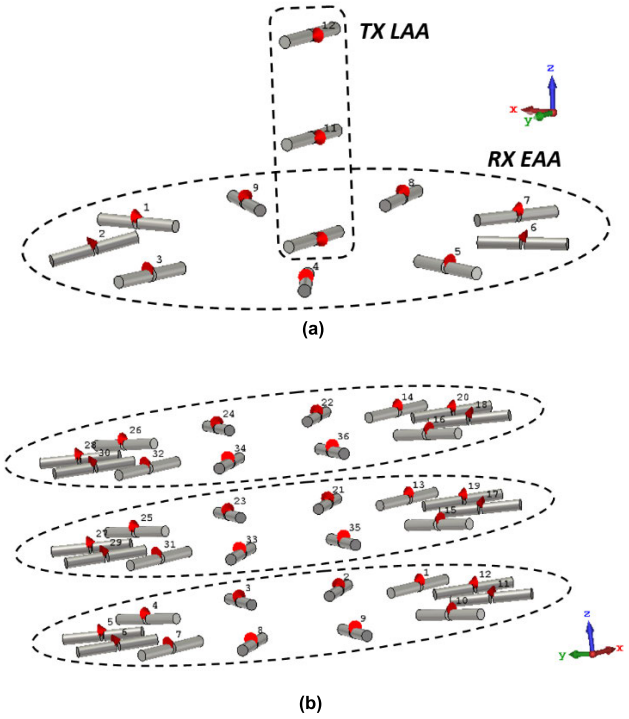

FIGURE 16. The elements distribution of (a) 12-elements UV-ECAA and (b) 36-elements U-ECAA using CST.

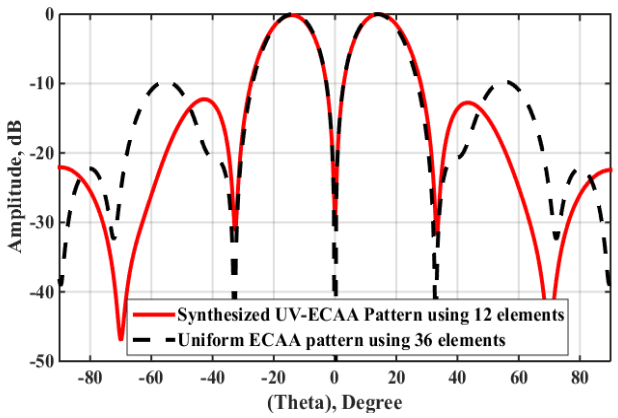

FIGURE 17. Rectangular plot of the U-ECAA pattern compared to the synthesized UV-ECAA pattern.

patterns are shown in Fig. 17. While, a comparison between the synthesized UV-ECAA and the U-ECAA in terms of HPBW, SLL, and number of elements is listed in Table 10. It is evident from the review of the data in Table 10 that the UV-ECAA and U-ECAA patterns have the same HPBW. However, the UV-ECAA has a lower SLL than that of the U-ECAA by 2.41 dB.

2) CST IMPLEMENTATION OF NUV-ECAA VERSUS NU-ECAA

In this section, the synthesized 13-element NUV-ECAA and 36-element NU-ECAA arrays introduced in section (IV.B) are implemented using the CST as shown in Fig. 18. Fig. 19 displays the rectangular patterns of the synthesized

TABLE 10. A comparison between the UV-ECAA pattern and the U-ECAA pattern in terms HPBW, SLL, and number of elements at f_o=0.305GHz.

Parameter	U-ECAA	UV-ECAA
HPBW	7.2°	7.2°
SLL	−9.7 dB	−12.11 dB
Number of elements	36	12

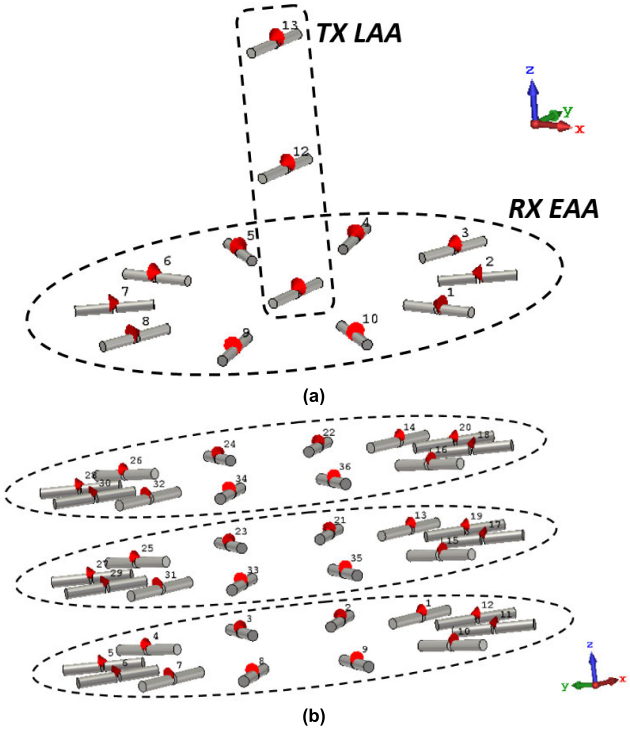

FIGURE 18. The elements distribution of (a) 13-elements NUV-ECAA and (b) 36-elements NU-ECAA using CST.

TABLE 11. A comparison between the NUV-ECAA pattern and the NU-ECAA pattern in terms HPBW, SLL, and number of elements at f_o = 0.305 GHz.

Parameter	NU-ECAA	NUV-ECAA
HPBW	10°	8.19°
SLL	−4.73 dB	−22.5 dB
Number of elements	36	13

NUV-ECAA and NU-ECAA. While the distinction between them in terms of HPBW, SLL, and number of elements is seen in Table 11. The results revealed that the NUV-ECAA has superior performance compared to the NU-ECAA in terms of HPBW and SLL, as it provides narrower HPBW by 1.81° and much lower SLL by 18.2 dB than the NU-ECAA. At the same moment, the NU-ECAA has a very high SLL equal to −4.73dB.

3) CST IMPLEMENTATION OF HBNUV-ECAA VERSUS HBNU-ECAA

In this section, we applied the HB on the implemented NUV-ECAA and NU-ECAA at $k = 0.5$ as an example. Fig. 20 shows the rectangular plot of the synthesized

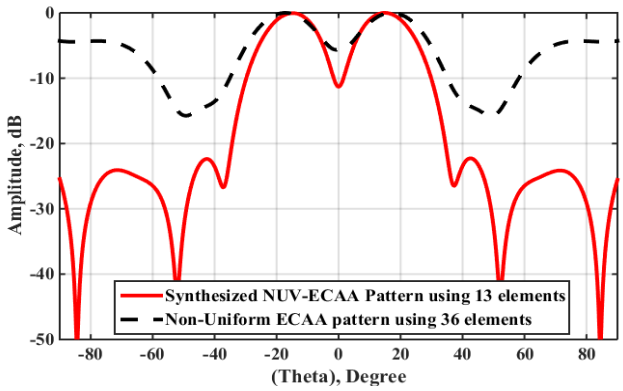

FIGURE 19. Rectangular plot of the synthesized NUV-ECAA pattern compared to the NU-ECAA pattern.

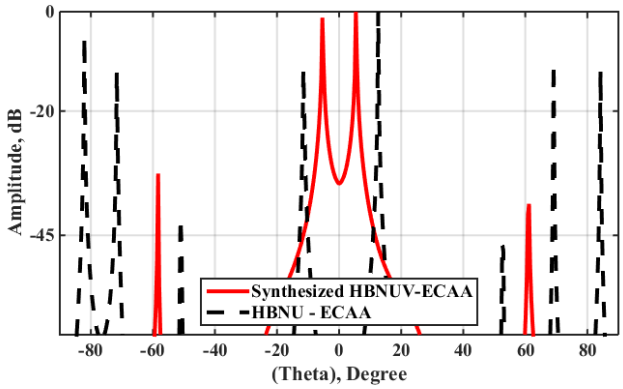

FIGURE 20. Rectangular plot of the synthesized HBNUV-ECAA pattern compared to the HBNU-ECAA pattern at $k = 0.5$.

TABLE 12. A comparison between the proposed HBNUV-ECAA patterns and the traditional HBUN-ECAA Patterns at $f_o = 0.305$ GHz.

Parameter	HBNU-ECAA	HBNUV-ECAA
HPBW	1°	1°
SLL	-5 dB	-32.5 dB

HBNUV-ECAA pattern compared to the HBNU-ECAA pattern at $k = 0.5$. The two arrays provide the same HPBW of 1°. While the synthesized HBNUV-ECAA has a SLL of -32.5 dB that is much lower than the HBNU-ECAA, which equals -5 dB as listed in Table 12.

VII. CONCLUSION

In this paper, the combination between VAA and PSO is utilized to improve the properties of the traditional ECAA in terms of SLL and HPBW, thereby the array directivity, gain, and the receiver sensitivity are significantly improved. The VAA is used to decompose the single transmit/receive ECAA into a separate transmit linear antenna array (LAA) and receive elliptical antenna array (EAA). While PSO is used to optimize the number of antenna elements, element spacing, and excitations of the LAA and EAA. In the case of uniform feeding, the proposed UV-ECAA provides an identical pattern to that of the uniform feeding ECAA using 66.6% fewer number of antenna elements. While in case of non-uniform feeding, the proposed NUV-ECAA provides better results than that of the non-uniform ECAA in terms of SLL and HPBW and saves 63.8% of the antenna elements. In case of applying the hyper beamforming, the simulation results revealed that the proposed HBV-ECAA provides significant reductions in the SLL and HPBW at different values of hyper beam exponent for both uniform and non-uniform feeding. In addition, the CST simulation results revealed that the synthesized V-ECAAs have superior performance compared to the traditional ECAAs in cases of uniform and non-uniform feeding. The implemented V-ECAAs provide much lower SLL and narrower HPBW than those of the implemented ECAAs.

REFERENCES

[1] S. U. Rahman, Q. Cao, M. M. Ahmed, and H. Khalil, "Analysis of linear antenna array for minimum side lobe level, half power beamwidth, and nulls control using PSO," *J. Microw., Optoelectron. Electromagn. Appl.*, vol. 16, no. 2, pp. 577–591, Apr. 2017.

[2] A. Das, D. Mandal, S. P. Ghoshal, and R. Kar, "An efficient side lobe reduction technique considering mutual coupling effect in linear array antenna using BAT algorithm," *Swarm Evol. Comput.*, vol. 35, pp. 26–40, Aug. 2017.

[3] S. A. Babale, D. D. Dajab, and K. Ahmad, "Synthesis of a linear antenna array for maximum side-lobe level reduction," *Int. J. Comput. Appl.*, vol. 85, no. 16, pp. 24–28, Jan. 2014.

[4] A. H. Hussein, H. H. Abdullah, A. M. Salem, S. Khamis, and M. Nasr, "Optimum design of linear antenna arrays using a hybrid MoM/GA algorithm," *IEEE Antennas Wireless Propag. Lett.*, vol. 10, pp. 1232–1235, 2011.

[5] G. Ram, D. Mandal, R. Kar, and S. P. Ghoshal, "Optimized hyper beamforming of receiving linear antenna arrays using firefly algorithm," *Int. J. Microw. Wireless Technol.*, vol. 6, no. 2, pp. 181–194, Apr. 2014.

[6] G. Ram, D. Mandal, R. Kar, and S. P. Ghosal, "Seeker optimization algorithm for beamforming of linear antenna arrays," in *Proc. 6th Int. Conf. Comput. Intell. Commun. Netw.*, Nov. 2014, pp. 14–16.

[7] G. Ram, D. Mandal, R. Kar, and S. P. Ghoshal, "Optimized hyper beamforming of linear antenna arrays using collective animal behaviour," *Sci. World J.*, vol. 2013, pp. 1–13, Jan. 2013.

[8] W. Q. Wang, "Virtual antenna array analysis for MIMO synthetic aperture radars," *Int. J. Antennas Propag.*, vol. 12, pp. 1–11, Jan. 2012.

[9] K. Sultan, H. Abdullah, E. Abdallah, and H. El-Hennawy, "MOM/GA-based virtual array for radar systems," *Sensors*, vol. 20, no. 3, pp. 1–16, Jan. 2020.

[10] B. El Dosouky, A. H. Hussein Abdullah, and S. Khamis, "A new high-resolution and stable MV-SVD algorithm for coherent signals detection," *Prog. Electromagn. Res. M*, vol. 35, pp. 163–171, Jan. 2014.

[11] H. A. El-Dawi, S. A. Napoleon, and A. H. Hussein, "VAE/MPM/GA technique for DoA estimation using optimized antenna arrays," *Wireless Pers. Commun.*, vol. 92, no. 3, pp. 1271–1279, Feb. 2017.

[12] A. A. Yahia and H. M. Elkamchouchi, "Design of virtual antenna array for direction of arrival estimation using real antenna array system," in *Proc. 34th Int. Tech. Conf. Circuits/Syst., Comput. Commun. (ITC-CSCC)*, Jun. 2019, pp. 1–3.

[13] W. Li and Y. Zhao, "A null broadening beamforming method of virtual antenna array," in *Proc. IEEE/ACES Int. Conf. Wireless Inf. Technol. Syst. (ICWITS) Appl. Comput. Electromagn. (ACES)*, Mar. 2016, pp. 1–2.

[14] C. Dahl, I. Rolfes, and M. Vogt, "Comparison of virtual arrays for MIMO radar applications based on hexagonal configurations," in *Proc. Eur. Radar Conf. (EuRAD)*, Sep. 2015, pp. 1439–1442.

[15] G. G. Lema, G. T. Tesfamariam, and M. I. Mohammed, "A novel elliptical-cylindrical antenna array for radar applications," *IEEE Trans. Antennas Propag.*, vol. 64, no. 5, pp. 1681–1688, May 2016.

[16] S. Bennour, A. Sallem, M. Kotti, E. Gaddour, M. Fakhfakh, and M. Loulou, "Application of the PSO technique to the optimization of CMOS operational transconductance amplifiers," in *Proc. 5th Int. Conf. Design Technol. Integr. Syst. Nanosc. Era*, Mar. 2010, pp. 1–5.

[17] S. Sengupta, S. Basak, and R. Peters, "Particle swarm optimization: A survey of historical and recent developments with hybridization perspectives," *Mach. Learn. Knowl. Extraction*, vol. 1, no. 1, pp. 157–191, Oct. 2018.
[18] S. Jayaprakasam, S. K. A. Rahim, C. Y. Leow, T. O. Ting, and A. A. Eteng, "Multiobjective beampattern optimization in collaborative beamforming via NSGA-II with selective distance," *IEEE Trans. Antennas Propag.*, vol. 65, no. 5, pp. 2348–2357, May 2017.
[19] I. Nadeem and D. Y. Choi, "Study on mutual coupling reduction technique for MIMO antennas," *IEEE Access*, vol. 7, pp. 563–586, 2019.

HEBA SOLIMAN DAWOOD received the B.Sc. degree in electronics and electrical communications engineering and the M.Sc. degree from Tanta University, Egypt, in 2014 and 2018, respectively. Her current research interests include antenna arrays and digital beamforming techniques.

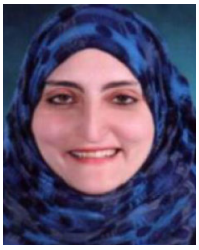

HEBA ALI EL-KHOBBY received the B.Sc. (Hons.), M.Sc., and Ph.D. degrees from the Faculty of Engineering, Tanta University, Tanta, Egypt, in 1998, 2003, and 2009, respectively. Since 2009, she has been a Teaching Staff Member with the Department of Electronics and Electrical Communications Engineering, Faculty of Engineering, Tanta University. Her current research interests include image enhancement, image restoration, image interpolation, super-resolution reconstruction of images, medical image processing, data hiding, multimedia communications, and wireless communications.

MUSTAFA MAHMOUD ABD ELNABY was a Visiting Professor with Kyushu University, Japan, working in design and fabrication of MOS devices for flash memory and communication systems applications. He was the Head of the Department of Electronics and Communication Engineering, Faculty of Engineering, Tanta University. He also served as a Visiting Professor with Aachen University, Germany, and Virginia Tech, VA, USA, in the area of electronics devices modeling and applications in digital communication systems. Since 2001, he has been a Professor of electrical engineering with the University of Qatar, Qatar. He is currently an Emeritus Professor with the Department of Electronics and communications Engineering, College of Engineering, Tanta University, Egypt. He has authored or coauthored more than 120 articles in the area of electronics and communication engineering. He was given several awards. He acts as a reviewer and a member of the editorial board for several scientific journals. His research interests include semiconductor devices, digital communication systems, nanotechnology, and biomedical engineering. He is currently the Head of the Permanent Scientific Committee for the promotion of professors and assistant professors with the Supreme Council of Universities.

AMR HUSSEIN HUSSEIN received the B.Sc. degree in electronics and electrical communications engineering from Tanta University, Egypt, in 2001, and the M.Sc. and Ph.D. degrees from Tanta University, in 2007 and 2012, respectively. His Ph.D. is devoted to introducing new MoM/GA based algorithms for different digital beamforming applications which are of main concern in the recent and future wireless communication systems. In 2017, he was an Associate Professor with Tanta University. He has also introduced VHDL implementations of both DOA estimation algorithms and the fixed beamwidth electronic scanning (FBWES) algorithm.